

# SECONDARY CELL WALL POLYMERS STUDIED BY CONFOCAL RAMAN MICROSCOPY: SPATIAL DISTRIBUTION, ORIENTATION, AND MOLECULAR DEFORMATION\*

N. GIERLINGER<sup>†</sup> and I. BURGERT

Max-Planck-Institute of Colloids and Interfaces,  
Department of Biomaterials, Am Mühlenberg 1, D-14471 Potsdam, Germany

(Received for publication 28 October 2005; revision 7 February 2006)

## ABSTRACT

Confocal Raman microscopy was used for chemical imaging of wood cell wall polymers and to follow molecular changes during tensile deformation. Spectral maps were acquired from cross-sections of poplar wood and images calculated by integrating the intensity of characteristic spectral bands. This enabled direct visualisation of the spatial variation of the lignin content without any chemical treatment or staining of the cell wall. A higher lignin content was visualised in the cell corners, the compound middle lamella, and the secondary cell wall of vessels than in the fibres. The S1 was distinguished from the S2 by integrating over the band at  $1097\text{ cm}^{-1}$ , because the intensity of this vibration is sensitive to the orientation of the cellulose molecule. The position of this band was shifted towards shorter wavenumbers during straining of wet tangential sections, demonstrating that the cellulose molecule was subjected to a deformation. The band shift was followed during the tensile test and a good trend and correlation with strain and stress were observed. Investigating tissue types with different properties and cell wall assemblies will help to reveal the polymer composition and orientation non-destructively with a high spatial resolution. By investigating structural changes during tensile straining, we aim at understanding the different stress-strain behaviour and the molecular mechanistic phenomena involved.

**Keywords:** Raman imaging; lignin distribution; cellulose orientation; microtensile testing; microdeformation; *Populus* sp.

## INTRODUCTION

While primary cell walls are adapted to allow cell growth, secondary cell walls preserve cell wall rigidity after cell death. To gain the required rigidity, thick cell

---

\* Based on a paper presented at 1st Joint New Zealand - German Symposium on Plant Cell Walls, 23–24 June 2005, Rotorua, New Zealand

<sup>†</sup> Corresponding author: Notburga.Gierlinger@mpikg.mpg.de

walls are made up of oriented cellulose microfibrils, embedded in a matrix of lignin and hemicelluloses. In wood these cell walls are highly structured, composed of several layers built at different periods during cell differentiation. The middle lamella found between the wood cells ensures the adhesion of a cell to its neighbours and is made up of pectic substances and lignin. Attached to the middle lamella is the primary cell wall (0.1  $\mu\text{m}$ ) on which, after reaching the definitive size, the secondary cell wall is formed (Plomion *et al.* 2001). This is the most important layer in terms of mechanical properties and it is divided into three — S1, S2, S3 — with different orientation of the cellulose microfibrils. The S2 layer is the thickest (75% to 85% of the total thickness of the cell wall) and with regard to mechanical support the most important one. The chemical composition and alignment of the microfibrils within the cell wall layers (especially S2) are highly variable in wood, showing differences among trees, but also within a single tree and within the annual ring during a growing season (Barnett & Bonham 2004).

To generate chemical images *in situ* from biological tissues brings a wealth of information, as it is not solely a chemical analysis of the sample *per se*, but of the intact tissue in context with the anatomy and spatial distribution within the sample. Infrared and Raman spectroscopy have been established in recent years as chemical mapping and imaging techniques for biological and biomimetic samples (Salzer *et al.* 2000; Chenery & Bowring 2003). Both methods are based on the discrete vibrational transitions that take place in the ground electronic state of molecules. Raman scattering involves excitation of a molecule with a photon of light (laser source) that is then scattered with a change in energy from the excitation photon, whereas infrared absorption spectroscopy typically involves absorption of an infrared photon of light from a lower vibrational energy level to a higher vibrational energy level. Raman scattering depends on changes in the polarisability of functional groups as the molecule vibrates, and infrared absorption depends on changes in the intrinsic dipole moments with molecular vibrations. Therefore Raman and Infrared spectroscopy can provide similar, but also complementary information about the vibrations of the molecule, and have different pros and cons. Advantages of Raman microspectroscopy are that spectra can be more easily acquired on aqueous, thicker samples and a higher spatial resolution can be achieved. Both techniques have developed as important tools in plant cell wall research (e.g., Atalla & Agarwal 1985; McCann *et al.* 1992; Séné *et al.* 1994; Stewart 1996; Himmelsbach *et al.* 1999; Kacuráková *et al.* 2000; McCann *et al.* 2001; Morris *et al.* 2003; Toole *et al.* 2004), as they allow direct information concerning the molecular structure and composition of undisrupted plant tissue.

Raman spectroscopy has also been used for evaluating changes that occur in samples subjected to stress and strain. Micromechanical studies have been conducted on polymeric fibres (e.g., Yeh & Young 1999; Davies *et al.* 2004) as well as on

various forms of cellulose and wood (e.g., Eichhorn *et al.* 2001, 2003; Kong & Eichhorn 2005; Sturcova *et al.* 2005). It was shown that during tensile deformation in cellulose fibres and cellulose composite systems (wood and paper) the  $1095\text{ cm}^{-1}$  Raman band, corresponding to the stretching of the cellulose ring structure, shifts towards a lower wavenumber due to molecular deformation. This effect is indicative of the stress in the fibres, and an invariant shift rate with stress in various cellulosic fibres (no matter what supposed crystal structure or specific mechanical properties) was observed (Eichhorn *et al.* 2001).

In this study confocal Raman microscopy was applied for chemical imaging on poplar wood and in combination with a tensile test device for monitoring molecular changes during deformation. The lignin distribution and cellulose orientation are followed across different cell wall layers by integrating over selected bands assigned to the wood polymers. An analysis of the spectra from selected areas further revealed details about differences in molecular structure and composition between and within cell wall layers. The molecular deformation was followed simultaneously during the tensile test and thus allowed us to monitor *in situ* the stretching of the cellulose molecule.

## MATERIALS AND METHODS

Samples were taken from near the cambium of a 27-year-old poplar tree (*Populus* sp.). Without any embedding routine, 20- $\mu\text{m}$ -thick cross-sections for chemical imaging and 80- $\mu\text{m}$ -thick tangential sections for tensile tests were cut on a rotary microtome (LEICA RM2255, Germany). For chemical imaging, samples were placed in water and sealed between a glass slide and a coverslip to prevent drying during measurement. For the deformation studies, the wet tangential sections were glued between foliar frames (testing length about 12 mm, width 2 mm), which afterwards were mounted on the crossheads of a tensile test device. The tensile apparatus was specially designed to measure mechanical properties and acquire spectra simultaneously. It consisted of a DC-motor driven at high-resolution stage permitting a wide range of feed rates, and a load cell with a capacity of 50 N. Synchronised force and elongation data were recorded during the measurement. Stress-strain diagrams were calculated by taking the sample dimensions (measured with a caliper) and the compliance of the setup into consideration.

Using a Confocal Raman Microscope (CRM200, WITEC, Germany) equipped with a piezo scanner (P-500, Physik Instrumente) and microscope objectives from Nikon ( $\times 100$  oil NA = 1.25 for imaging,  $\times 60$  water NA = 1.0 for deformation studies) spectra were acquired. A linear polarised laser (diode pumped Green laser,  $\lambda = 532\text{ nm}$ , CrystaLaser) was focused with a diffraction-limited spot size ( $0.61\lambda/\text{NA}$ ) and the Raman light was detected by an air-cooled, back-illuminated

spectroscopic CCD (ANDOR) behind a grating (600 g/mm) spectrograph (ACTON). The electric vector of the laser was in the x-direction during imaging and in the axial sample direction (parallel to the fibres) during tensile testing. For the imaging, spectra were taken every 0.25  $\mu\text{m}$  with an integration time of 2s (160  $\times$  160 spectra on a 40  $\mu\text{m}$   $\times$  40  $\mu\text{m}$  area). During the tensile test an integration time of 30s was chosen to get definitive band positions from every single spectrum acquired during the tensile test. Due to the straining of the section, position and focus changed and refocusing was required after almost every measurement.

The ScanCtrlSpectroscopyPlus software (WITEC, Germany) was used for measurement setup and image processing. Chemical images were achieved by using a sum filter, integrating over defined bands in the wood spectrum. The filter calculates the intensities within the chosen range and the background is subtracted by taking the baseline from the first to the second border. The scale of all images goes from black (no signal) to yellow (high intensity). With the help of the chemical images cell wall layers could be separated, and defined cell wall areas were marked to calculate average spectra from the selected area. As the cell wall layers have different proportions, the selected areas have different sizes and thus the number of spectra, used for calculation of average spectra, changes. The average and single spectra were analysed with the OPUS software package (Version 5.5). Band position of the single spectra acquired during tensile tests were calculated after a 9pt smoothing.

## RESULTS AND DISCUSSION

### Chemical Imaging

Fibres adjacent to a vessel on a cross-section of poplar wood were investigated. Chemical images were calculated by integrating over defined bands observed in the wood spectra (Fig. 1). Integrating from 1543 to 1814  $\text{cm}^{-1}$ , a region dominated by the aromatic C=C vibration of lignin at 1600  $\text{cm}^{-1}$  (Agarwal & Ralph 1997), allows the lignin distribution within the sample to be visualised (Fig. 2A). Especially the lignin-rich cell corner (CC) and the compound middle lamella (CML, middle lamella, and primary wall) are emphasised, whereas within the S2 less lignin is observed. The S2 of the vessel shows higher intensity than the S2 of the fibres. Integrating over the strong band at 2898  $\text{cm}^{-1}$  emphasises more the cellulose-rich regions, in particular the S2 (Fig. 2B). Nevertheless, differences in intensity are observed between the S2 of the big cells and small cells (fibres marked with \*, Fig. 2B) and the S2 of the vessels. Taking the small range from 1079 to 1114  $\text{cm}^{-1}$ , comprising the C-O-C stretching vibration of cellulose, allows a small layer of about 0.5  $\mu\text{m}$  (S1) in the radial (x-) direction (Fig. 2C) to be distinguished. Higher intensity was also observed in the S2 of the vessel walls.

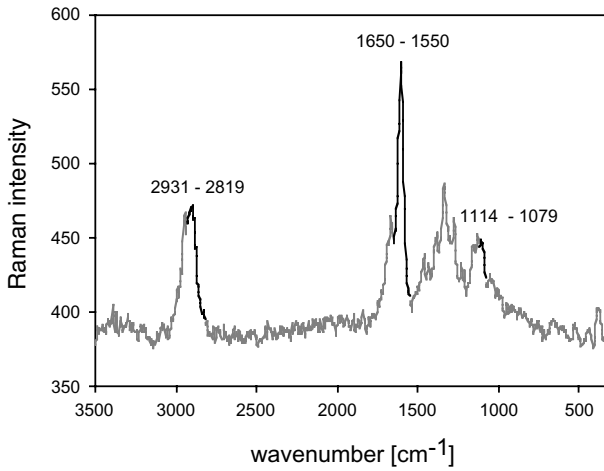


FIG. 1—Average Raman spectrum of poplar wood calculated from the whole cross-section. The black marked ranges correspond to the wavenumber regions used for calculating the chemical images shown in Fig. 2A–C.

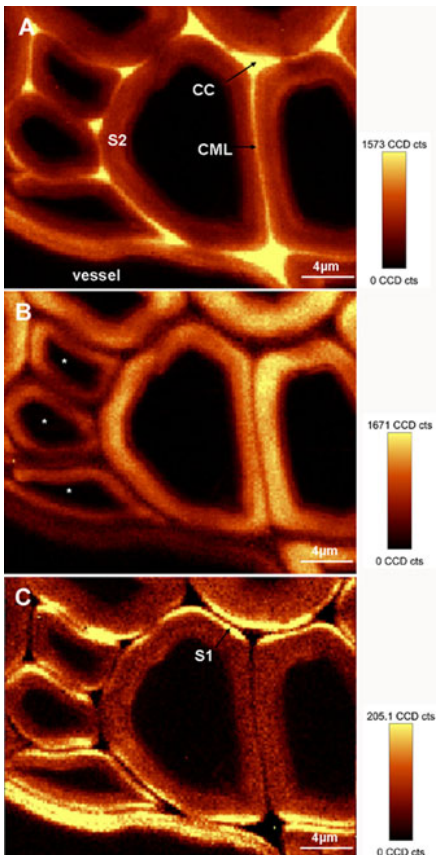


FIG. 2A–C: Raman images of a cross-section of poplar wood showing the intensity of the aromatic lignin band (A, 1650 to 1550 cm<sup>-1</sup>), the CH and CH<sub>2</sub> stretching of cellulose (B, 2931 to 2819 cm<sup>-1</sup>), and the 1100 cm<sup>-1</sup> band (C, 1114 to 1079 cm<sup>-1</sup>).

Marking the distinguished cell wall layers (CC, S2, S2 vessel, S2 small cells, S1) on the chemical images and calculating average spectra allows more detailed information on the differences to be gained (Fig. 3A–B). In the CC spectrum a higher fluorescence background (causing a shift in the Raman intensity axis) is observed, which is due to the higher lignin content, also seen in the higher peak at  $1600\text{ cm}^{-1}$  (Fig. 3A). Spectra of the S2 of the vessel wall and the S1 of the fibres look similar and show also a higher background and stronger lignin signals than the S2

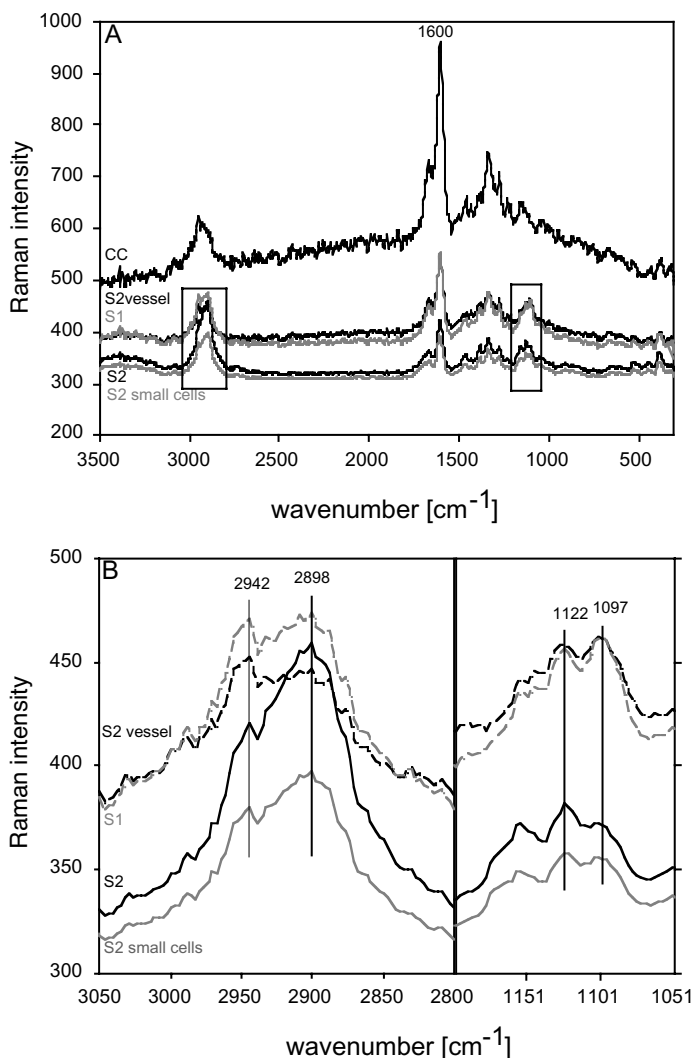


FIG. 3A–B: Average Raman spectra of the cell corner (CC), the S2 of the fibres (S2), of the vessel (S2vessel), the small cells (S2 small cells), and of the distinguished S1 layer (S1) (A). Zoom into regions of interest (B).

of the fibre walls. In the C-H stretching region (2975 to 2840  $\text{cm}^{-1}$ ) in the CC spectrum the peak at 2942  $\text{cm}^{-1}$  from the stretching of the methoxyl groups of the lignin is more pronounced, whereas in the S2 the peak at 2898  $\text{cm}^{-1}$ , attributed to C-H stretching of cellulose, dominates (Fig. 3A). In the S2 and S1 spectra the bands at 1122  $\text{cm}^{-1}$  and 1097  $\text{cm}^{-1}$ , assigned to symmetric and antisymmetric stretching of C-O-C linkages (Edwards *et al.* 1997) of cellulose, are more pronounced than in the CC spectrum (Fig. 3A). A zoom into the CH, CH<sub>2</sub> stretching region and into the CC, CO stretching region shows changed band height ratios in the S2 and S1 spectra (Fig. 3B). In the S2 of the vessel and the S1 of the fibres the band at 2898  $\text{cm}^{-1}$  is strongly reduced (compared to the 2942  $\text{cm}^{-1}$  band), and the band at 1097  $\text{cm}^{-1}$  (compared to the band at 1122  $\text{cm}^{-1}$ ) is increased. The changed band height ratios are in context with the orientation of the cellulose molecule, as bands deriving from perpendicular oriented C-H-bonds decrease (symmetric str. 2898  $\text{cm}^{-1}$ ), while the parallel oriented C-O-C (1097  $\text{cm}^{-1}$ ) increase (Agarwal & Atalla 1986). These two bands were recognised to be highly sensitive to the orientation in cellulose (Wiley & Atalla 1987) and consequently allowed layers with different microfibril angle to be distinguished within the secondary cell wall (Fig. 1C). For *Fagus crenata* the average fibrillar angle in a vessel wall was reported to be about 50° to 70°, whereas the angles in the tracheids and fibres were small (Harada 1965). In the S1 the fibrils are known to run with a gentle helical slope (Fengel & Wegener 1989) and therefore the vessels as well as the S1 showed a change in the orientation sensitive 1097  $\text{cm}^{-1}$  band. This was observed only on the radial walls in the x-direction of the image, because the laser beam was polarised in x-direction. Turning the sample 90° would emphasise the signal in the S1 of the tangential walls. The small changes observed between “normal” fibres and “small fibres” (representing fibre ends) suggest a less steep orientation of the cellulose molecules at the fibre ends.

Because of the multicomponent nature of wood its vibrational spectrum is rather complex with broad overlapping bands. Cellulose and hemicelluloses have similar chemical bonds and are therefore difficult to discern (Agarwal & Ralph 1997). Generally the skeletal motions of most of the hemicelluloses result in fairly broad bands, unless they are so organised that they have a high degree of repetitive order.

Lignin because of its aromatic nature shows up with a sharp, strong contribution around 1600  $\text{cm}^{-1}$ , which enabled imaging of the lignin distribution by integrating over this wavenumber area (Fig. 2A). Lignin distribution has been studied in the xylem of gymnosperms and angiosperms using a variety of techniques, such as UV microscopy (e.g., Koch & Kleist 2001), energy dispersive X-ray analysis (e.g., Westermark *et al.* 1988), interference and fluorescence microscopy (e.g., Donaldson *et al.* 2001). Using Raman microscopy allows the samples to be investigated *in situ* without any staining or chemical pre-treatment and besides the lignin distribution (Fig. 2A) information on the polymer nature and orientation can be gained

(Fig. 2C). A lot of information is hidden behind the images in the spectra; small changes in band positions and intensities can give information about changes in polymer composition and orientation. Nevertheless, the wealth of information embedded in the spectra is not readily accessible as many factors (amount, composition, orientation, crystallinity, linkage to other components) contribute to the spectral changes.

### Tensile Testing Combined with Raman Microscopy

Spectra of the tangential section, acquired during the deformation studies, differed clearly from the spectra of the cross sections (Fig. 1, Fig. 4). As the fibre orientation is now parallel to the electric vector of the laser beam, the band at  $1097\text{ cm}^{-1}$  is

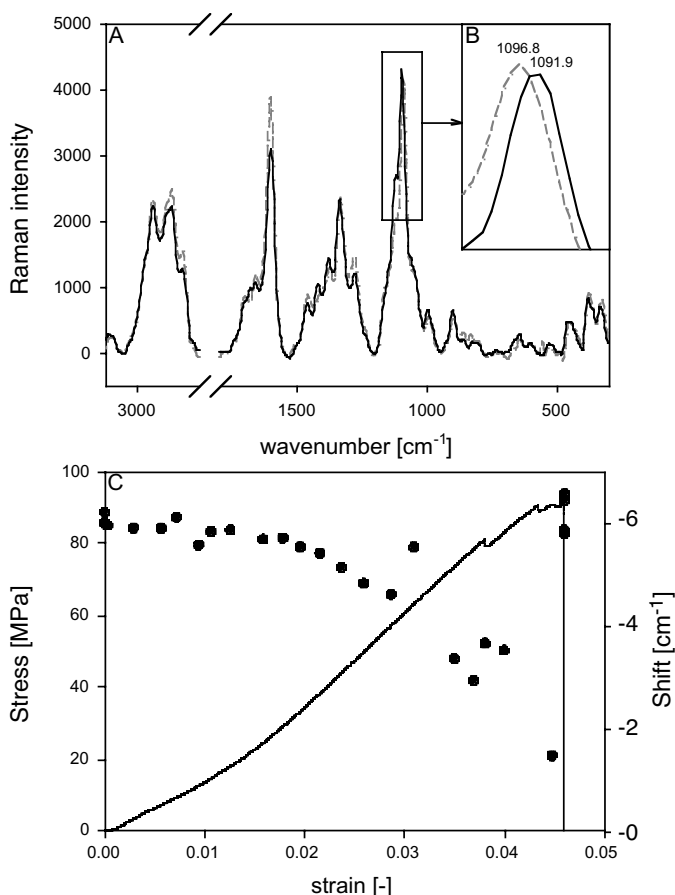


FIG. 4A–C: Raman spectra (smoothed 9pts, baseline corrected (bc)) acquired on tangential sections of poplar wood before (grey line) and during the tensile test (black line) (A), and a zoom into the strain-induced Raman shift of the  $1097\text{ cm}^{-1}$  band (B). Calculated band shifts ( $1097\text{ cm}^{-1}$ ) of all spectra during the tensile test together with the corresponding stress-strain curve (C).

increased and gets as high as the lignin band at  $1600\text{ cm}^{-1}$  (Fig. 4A). During the tensile test a clear shift of the  $1097\text{ cm}^{-1}$  band was observed down to  $1092\text{ cm}^{-1}$  before the sample ruptured (Fig. 4B, Fig. 4C). After sample failure the band was found again at its original position at  $1097\text{ cm}^{-1}$  (Fig. 4C). Changes in intensity and position were also observed for several other bands (Fig. 4B), but it was not possible to clearly distinguish between changes due to molecular deformation and due to deformation of the section and subsequent changes in the focus.

At low strain levels almost no change in the band position was observed, followed by a linear shift to lower wavenumbers (Fig. 4C, 5A). Comparing the band shifts of two samples with different stress-strain curves, shows that the regression line is rather similar when correlated with strain (Fig. 5A), but shows a different slope (less steep) when correlated with stress (Fig. 5B). Higher stress levels in the stiffer sample did not result in higher band shifts, but were in accordance with less strain. Thus, the strain determines more the extent of the band shift (stretching of the cellulose molecule) than the load taken up within different poplar samples.

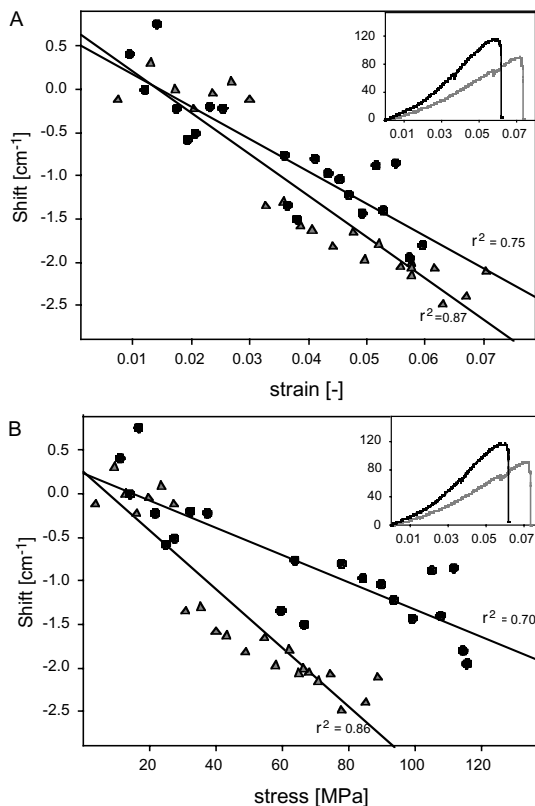


FIG. 5A–B: Correlations of the Raman band shift at  $1097\text{ cm}^{-1}$  with strain (A) and stress (B) of two poplar samples with different stress strain behaviour (*see* insert).

An earlier published study on wood reported high variability of the mean band shift which was explained by the fact that the laser spot cannot be focused on to one particular layer (S1, S2, S3) (Eichhorn *et al.* 2001). The problem of proper refocusing and resulting changes in the spectra has been noticed too; nevertheless the 1097  $\text{cm}^{-1}$  band shift showed a good correlation with strain and stress, and within one single tensile test (Fig. 4C, 5A,B). Improvements in the experiment set up are under way to evaluate other changes in the spectra.

## CONCLUSIONS

Raman microscopy is an invaluable tool in plant cell wall research as cell wall polymer composition and orientation can be investigated with a high lateral resolution, which enables different cell wall layers to be distinguished. Nevertheless, the wealth of information embedded in the spectra is not readily accessible as many factors (amount, composition, orientation, crystallinity, linkage to other components) contribute to the spectral changes. By making further investigations on different samples and model systems, better knowledge can be gained in spectra interpretation and the gathered information could be enlarged.

In addition, Raman microscopy allows the deformation of the cellulose molecule to be followed by the clear shift of the band at 1097  $\text{cm}^{-1}$  *in situ* during tensile tests. Future improvements of the experiment setup and investigations into tissues and fibres with different mechanical properties will allow more information to be gained on molecular mechanistic phenomena in plant cell walls.

## ACKNOWLEDGMENTS

We thank Dr H.S.Gupta (MPIKG Potsdam) for help with the tensile test device and Antje Reinecke (MPIKG Potsdam) for technical assistance.

## REFERENCES

- AGARWAL, U.P.; ATALLA, R.H. 1986: In-situ Raman microprobe studies of plant cell walls: Macromolecular organization and compositional variability in the secondary wall of *Picea mariana* (Mill.) B.S.P. *Planta* 169: 325–332.
- AGARWAL, U.P.; RALPH, S. 1997: FT-Raman spectroscopy of wood: Identifying contributions of lignin and carbohydrate polymers in the spectrum of black spruce (*Picea mariana*). *Applied Spectroscopy* 51: 1648–1655.
- ATALLA, R.H.; AGARWAL, U.P. 1985: Raman microprobe evidence for lignin orientation in the cell walls of native woody tissue. *Science* 227: 636–638.
- BARNETT, J.R.; BONHAM, V.A. 2004: Cellulose microfibril angle in the cell wall of wood fibres. *Biol Rev* 79: 461–472.
- CHENERY, D.; BOWRING, H. 2003: Infrared and Raman spectroscopic imaging in bioscience. *Spectroscopy Europe* 15: 8–14.

- DAVIES, R.J.; EICHHORN, S.J.; RIEKEL, C.; YOUNG, R.J. 2004: Crystal lattice deformation in single poly(p-phenylene benzobisoxazole) fibres. *Polymer* 45: 7693–7704.
- DONALDSON, L.; HAGUE, J.; SNELL, R. 2001: Lignin distribution in coppice poplar, linseed and wheat straw. *Holzforschung* 55: 379–385.
- EDWARDS, H.G.M.; FARWELL, D.W.; WEBSTER, D. 1997: FT Raman microscopy of untreated natural plant fibres. *Spectrochim Acta A* 53: 2383–2392.
- EICHHORN, S.J.; SIRICHAISIT, J.; YOUNG, R.J. 2001: Deformation mechanisms in cellulose fibres, paper and wood. *Journal of Materials Science* 36: 3129–3135.
- EICHHORN, S.J.; YOUNG, R.J.; DAVIES, R.J.; RIEKEL, C. 2003: Characterisation of the microstructure and deformation of high modulus cellulose fibres. *Polymer* 44: 5901–5908.
- FENGEL, D.; WEGENER, G. 1989: “Wood: Chemistry, Ultrastructure, Reactions.” Walter de Gruyter & Co., Berlin.
- HARADA, H. 1965: Ultrastructure of angiosperm vessels and ray parenchyma. Pp. 235–249 in Cote, W.A. (Ed.) “Cellular Ultrastructure of Woody Plants”. Syracuse University Press, Syracuse.
- HIMMELSBACH, D.S.; KHAHILI, S.; AKIN, D.E. 1999: Near-infrared–Fourier-transform–Raman microspectroscopic imaging of flax stems. *Vibrational Spectroscopy* 19: 361–367.
- KACURÁKOVÁ, M.; CAPEKA, P.; SASINKOVÁ, V.; WELLNER, N.; EBRINGEROVA, A. 2000: FT-IR study of plant cell wall model compounds: pectic polysaccharides and hemicelluloses. *Carbohydrate Polymers* 43: 195–203.
- KOCH, G.; KLEIST, G. 2001: Application of scanning UV microspectrophotometry to localise lignins and phenolic extractives in plant cell walls. *Holzforschung* 55: 563–567.
- KONG, K.; EICHHORN, S.J. 2005: Crystalline and amorphous deformation of process-controlled cellulose-II fibres. *Polymer* 46: 6380–6390.
- McCANN, M.C.; HAMMOURI, M.; WILSON, R.H.; BELTON, P.; ROBERTS, K. 1992: Fourier Transform Infrared Microspectroscopy is a new way to look at plant cell walls. *Plant Physiology* 100: 1940–1947.
- McCANN, M.C.; BUSH, M.; MILIONIA, D.; SADOA, P.; STACEY, N.J.; CATCHPOLE, G.; DEFERNEZ, M.; CARPITA, N.C.; HOFT, H.; ULVSKOV, P.; WILSON, R.H.; ROBERTS, K. 2001: Approaches to understanding the functional architecture of the plant cell wall. *Phytochemistry* 57: 811–821.
- MORRIS, V.J.; RING, S.G.; MacDOUGALL, A.J.; WILSON, R.H. 2003: Biophysical characterisation of plant cell walls. Pp. 1513–1523 in Rose, J. (Ed.) “The Plant Cell Wall — Annual Plant Reviews”.
- PLOMION, C.; LEPROVOST, G.G.; STOKES, A. 2001: Wood formation in trees. *Plant Physiology* 127: 1513–1523.
- SALZER, R.; STEINER, G.; MANTSCH, H.H.; MANSFIELD, J.; LEWIS, E.N. 2000: Infrared and Raman imaging of biological and biomimetic samples. *Fresenius Journal of Analytical Chemistry* 366: 712–726.
- SÉNÉ, C.F.B.; McCANN, M.C.; WILSON, R.H.; CRINTER, R. 1994: Fourier-Transform Raman and Fourier-Transform Infrared Spectroscopy. An investigation of five higher plant cell walls and their components. *Plant Physiology* 106: 1623–1631.

- STEWART, D. 1996: Fourier Transform Infrared Microspectroscopy of plant tissues. *Applied Spectroscopy* 50: 357–365.
- STURCOVA, A.; DAVIES, G.R.; EICHHORN, S.J. 2005: Elastic modulus and stress-transfer properties of tunicate cellulose whiskers. *Biomacromolecules* 6: 1055–1061.
- TOOLE, G.A.; KACURÁKOVÁ, M.; SMITH, A.C.; WALDRON, K.W.; WILSON, R.H. 2004: FT-IR study of the *Chara corallina* cell wall under deformation. *Carbohydrate Research* 339: 629–635.
- WESTERMARK, U.; LIDBRANDT, O.; ERIKSSON, I. 1988: Lignin distribution in spruce (*Picea abies*) determined by mercurization with SEM-EDXA technique. *Wood Science Technology* 22: 243–250.
- WILEY, J.H.; ATALLA, R.H. 1987: Band assignment in the raman spectra of celluloses. *Carbohydrate Research* 160: 113–129.
- YEH, W.-Y.; YOUNG, R.J. 1999: Molecular deformation processes in aromatic high modulus polymer fibres. *Polymer* 40: 857–870.